Macromolecular Research, Vol. 14, No. 2, pp 187-193 (2006)

Structure and Properties of the Organoclay Filled NR/BR Nanocomposites

Wonho Kim*, Sang Kwon Kim, Jong-Hyub Kang, and Youngsun Choe

Department of Chemical Eng., Pusan National University, Busan 609-735, Korea

Young-Wook Chang

Department of Chemical Eng., Hanyang University, Ansan 425-791, Korea

Received November 3, 2005; Revised January 18, 2006

Abstract: Organoclay, was applied as a filler, in place of carbon black and silica, to a natural rubber (NR)/butadiene rubber (BR) blend. A compounding method was used to disperse and separate the layered silicates. The effect of a coupling agent on the vulcanizates was evaluated using both the silica and organoclay filled compounds. After the compounding processes were completed, the XRD diffraction peaks disappeared, but then reappeared after vulcanization. The scorch times for the organoclay-filled compounds were very short compared to those for carbon black and silica-filled compounds. The organoclay-filled compounds showed high values of tensile strength, modulus, tear energy, and elongation at the break. When ranked by viscosity, the compounds appeared in the following order: silica > silica (Si-69) > organoclay > organoclay (Si-69) > carbon black. Fractional hysteresis, tensile set, and wear rates were very consistent with the viscosity of the vulcanizates. The Si 69 coupling agent increased reversion resistance, the maximum torque values in the ODR, modulus, and wear resistance, but decreased elongation at the break, fractional hysteresis, and tension set of the vulcanizates.

Keywords: organoclay, NR/BR nanocomposites, coupling agent.

Introduction

Active development of nanotechnology began in the 1990's in all fields of science and engineering. Since organoclay was introduced to polyamide by the Toyota group,[1,2] many researchers have studied a variety of polymer nanocomposites using organoclay. Clays such as montmorillonite are composed of silicate layers. The dimensions of the silicates are, approximately, 1 nm thickness and 100-1,000 nm in the lateral dimensions. Dispersion of such clays into polymeric materials is very difficult because of their hydrophilic nature, i.e., formation of aggregates in the hydrophobic matrix. Inorganic cations such as Na^+, Ca^{++}, and K^+ exist in the galleries of silicate layers, and can be exchanged by quaternary alkyl ammonium ions, which make the silicates compatible with the polymeric matrix and produce nanocomposites by exfoliating the layered silicates during the compounding processes. When the organoclay was exfoliated in the nanocomposites, the silicates had an aspect ratio of more than one hundred and a very large specific surface area. Due to these characteristics, small amounts of nanoclay filled composites have the following excellent physical and mechanical properties: increased modulus, tensile, flexural properties, and heat distortion temperature, as well as decreased gas permeability and flammability.[3]

Until recently, relatively little attention has been paid to rubber nanocomposites though a variety of properties can be improved by reinforcing them with nanoclay.

Preparations for rubber matrix nanocomposites can be classified as follows: the solution methods,[4-8] the compounding methods,[9-17] and the latex methods.[18-23] The advantages of the compounding methods are that conventional processing equipments can be used and the methods are environmentally friendly. Due to the presence of long alkyl chains in the galleries of silicate layers, the silicate surface became less hydrophilic and the interlayer distance increased. This leads to increased dispersion of clays in the rubber matrix and reduced agglomeration of clays. Studies of nanocomposites prepared with the compounding methods have used natural rubber (NR),[9-11] butadiene rubber (BR),[12,13] styrene butadiene rubber (SBR),[12] nitrile butadiene rubber (NBR),[14,15] ethylene propylene rubber (EPR),[16] ethylene propylene diene rubber (EPDM),[17] and other types of rubber. These rubber nanocomposites have excellent modulus, tensile strength, elongation at the break, and tear strength with small amounts of organoclay.

*Corresponding Author. E-mail: whkim@pnu.edu

The NR(35 phr)/BR(65 phr) blend had a good balance between mechanical strength and wear resistance for rubber outsoles in footwear. This paper describes a study of NR (35 phr)/BR(65 phr) blend loaded with organoclay, carbon black, silica, and Na-MMT. Organoclay, which is substituted with dimethyl dihydrogenatetallow ammonium, is dispersed in the NR/BR blend by using a Banbury mixer and a two-roll mill. Interlayer spacing by mixing time in a Banbury mixer was determined by XRD. Also spacing was determined after compounding and after vulcanization. After vulcanization, the morphologies of the organoclay were characterized by transmission electron microscopy (TEM). The cure characteristics, mechanical properties, hysteresis and wear resistance of the organoclay filled nanocomposites were evaluated and compared to carbon black or silica filled compounds.

Experimental

Materials. SVR-3L for NR and KBR-01 (Mol. wt., 250,000, Mooney viscosity ML 1+4(100 °C) 45, cis-1,4-polybutadiene 96%) for BR were used as base rubbers. Carbon black (ISAF, N220), silica (Zeosil-155), Na-MMT (Kunipia, Japan), and organoclay (Cloisite 15A, Southern Clay Products, USA) were used as fillers, and the content was restricted to 10 phr of the NR/BR blend. The first compounding additives were zinc oxide (ZnO), stearic acid, and paraffinic oil. The second compounding additives were sulfur, dibenzothiazyl disulfide (MBTS; trade name DM), and tetramethyl thiuram monosulfide (TMTM; trade name TS). BHT (2,6-di-*t*-butyl-4-methyl phenol) was used as an antioxidant and Si-69 (TESPT: bis(3-triethoxysilylpropyl)tetrasulfane) was used as a coupling agent.

Preparation of Samples. Base rubbers (35 phr of NR and 65 phr of BR) were blended by using a 10" two-roll mill at 60 °C for 3 min, after that fillers are mixed with base rubbers in the Banbury mixer (Haake Rheocord 300P, Germany) for 8 min at 80 °C. After that the compounds were returned to the two-roll mill, and compounded for an additional 5 min at 60 °C. Next, additives were mixed with the previous compounds using the two-roll mill for 10 min at 60 °C. To maximize the mixing efficiency, additives were added in the following sequence: ZnO, stearic acid, paraffinic oil, antioxidants, sulfur and accelerators. Optimum cure time (t90) for the compounds was determined by measuring the torque values of the unvulcanized compounds at 160 °C by using the Curometer (Myung Ji Tech., Korea, Model; ODR 2000). Vulcanizates were prepared by applying 190 bar using a hydraulic hot press at 160 °C for the optimum cure time. Experimental formulations are shown in Table I.

Test Methods. X-ray diffraction analysis was performed using a D/MAX 2200 diffractometer (Cu Kα radiation (λ= 0.154056 nm), Rigaku Co., Japan) and scanning at a rate of 1 °/min from 1.5 to 10.0 °. Bragg's law was used to calculate the basal distance (d); $\lambda=2d \sin \theta$. Tensile strength, elongation at the break, and 100 & 300% modulus of vulcanizates were measured by using dumbbell type specimens according to the ASTM D412. Universal testing machine (UTM, Instron 4485, USA) with a 1,000 N load cell and 500 mm/min of crosshead speed were used. Tearing energy was measured by the trouser tear test. Fractional hysteresis and the tension set were measured using a UTM with dumbbell shaped specimens. At 100% of elongation with an extended specimen, 5 min were allowed for stress relaxation, after that retraction was allowed at zero stress. This process was performed three times for the cyclic tension test. Abrasion resistance was measured by using a knife type abrasion tester (Ill Jin Technology, Korea). The specimens had the following dimensions: outer radius, 22 mm; inner radius, 6 mm; and thickness, 20 mm. The knife was used to apply a normal load (39.2 Newtons) to the specimen, after that, a preliminary abrasion was performed at a rotation speed of 12 rpm. After the abrasion pattern was formed on the surface of the specimen, the abrasion test was started.

Table I. Experimental Formulations **(Amount: phr)**

Code	C1	C2	C3	C3-1	C4	C5	C5-1
NR	35						
BR	65						
Filler	0	10	10	10	10	10	10
	Non-filler	C/B	Silica	Silica (Si-69)	Na-MMT	Organo-clay	Organo-clay (Si-69)
Si-69	0	0	0	1	0	0	1
ZnO	4						
S/A	1						
BHT	1						
Oil	5						
S	2						
MBTS	1.5						
TMTM	0.15						

Results and Discussion

XRD Patterns and Cure Characteristics of the NR/BR Compounds. Figure 1 shows the X-ray diffraction patterns of the Na-MMT and the organoclay. The Na-MMT shows a diffraction pattern peak at $2\theta=7.2°$, which corresponds to the average basal spacing (d-spacing) of 12.3 Å. In the organoclay, two peaks are shown. The first peak, which is the major peak, moved to lower angles, i.e., $2\theta=2.8°$. The basal spacing increased from 12.3 to 31.5 Å. This spacing indicates that long alkyl (dimethyl dihydrogenatetallow) ammonium ions were inserted into the gallery of Na-MMT, as a result, an intercalated structure formed. The inserted long alkyl chains

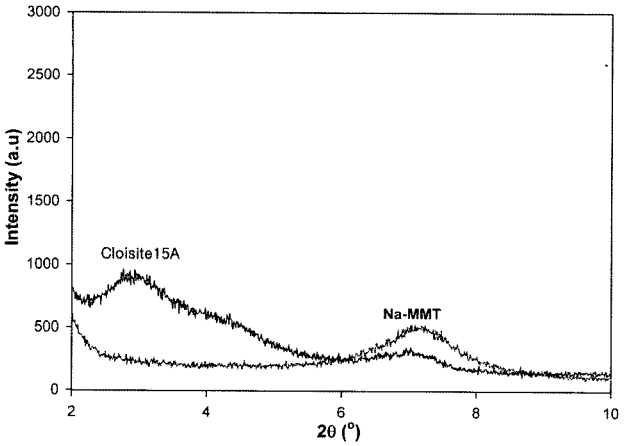

Figure 1. XRD patterns of organoclay (Cloisite 15A) and Na-MMT.

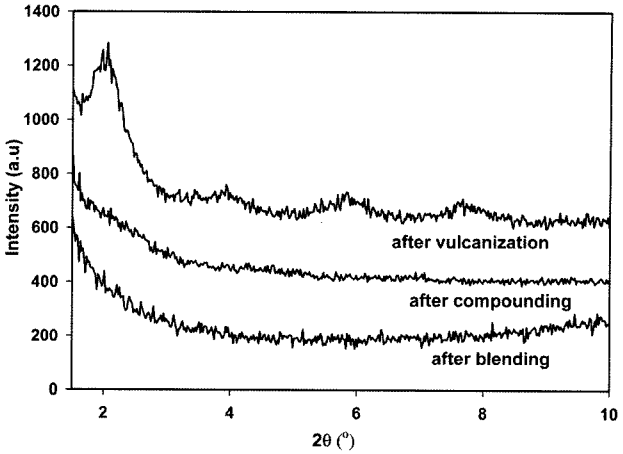

Figure 3. XRD patterns: after blending the NR/BR, and after compounding and vulcanization of the NR/BR nanocomposites.

caused the hydrophilic nature of the clay to decrease, and this effect improved the dispersion of silicates in the rubber matrix. The second peak is shown at 2θ=7.2°, which is same as the peak of the Na-MMT. This result indicates that some amounts of Na-MMT were not modified with alkyl ammonium ions.

Figure 2 shows the X-ray diffraction patterns of the organoclay in the NR/BR blend by mixing time. The diffraction pattern peaks should be at 2.8 and 7.2°, the same as those in the organoclay, when the compounding process starts.

The shift of 001 peak to the lower angles represents an increase in the distances between the silicate platelets. By comparing the diffraction patterns after 3 min of mixing with those of the organoclay, the first peak has moved from 2.8 to 2.1°. This shift suggests that the interlayer distance of silicates increased from 31.5 to 42.0 Å. At the fourth and fifth minute of mixing, the first and second peaks could not be distinguished with the main X-ray beam. This is due to the higher spacing of the silicate platelets.

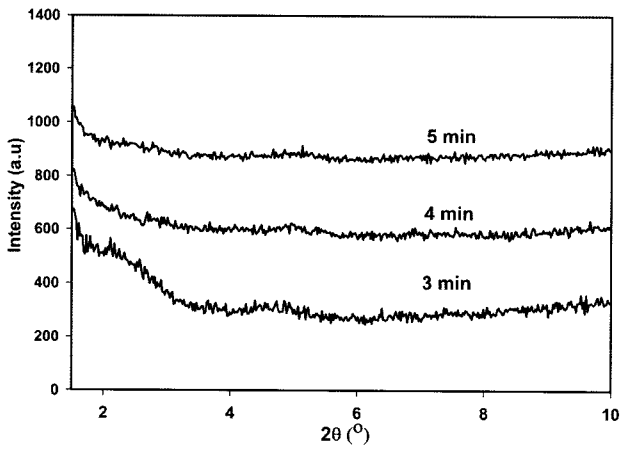

Figure 2. XRD patterns of organoclays filled NR/BR blend by mixing time in the Banbury mixer.

Figure 3 shows, the X-ray diffraction patterns of the NR/BR blends, the NR/BR compounds, and the NR/BR vulcanizates. After compounding, the XRD pattern did not show a characteristic 001 peak in the low angle range. This is due to the higher layer spacing of the silicates. Meanwhile, after vulcanization, a characteristic 001 peak reappeared at 2.0°, which corresponds to 44.1 Å of layer distance, and three other small peaks appeared. These ordered structures may be due to the escape or rearrangement of long chains of alkyl ammonium ions, which were inserted in the galleries of the organoclay, by the vulcanization reaction or by the high pressure applied during vulcanization. Varghese and Karger-Kocsis[10] emphasized that formation of the zinc-sulfur-amine complex during vulcanization resulted in reduced gallery distances.

Figure 4 shows examples of TEM micrographs of the Cloisite 15 A (Figure 4(a); scale bar: 50 nm) and the NR/BR nanocomposites (Figure 4(b); scale bar: 100 nm). The dark lines in the TEM image are the intersections of the silicate layers. For Cloisite 15 A, the thickness of the bundled layers, the number of silicates in the layers, and distance between silicates were 42~48 nm, 13~14 silicates, and 30~35 Å, respectively. The distance between silicates 30~35 Å is very consistent with the XRD result of 31.5 Å for Cloisite 15 A. As shown in Figure 4(b), organoclays are well dispersed in the rubber matrix and many parts of the organoclay in the NR/BR nanocomposites were separated from the original 13~14 layers to the 3~5 layers. Thus the surface area and the aspect ratio of the silicate layers increased.

To evaluate the effect of incorporation of the fillers on the cure characteristics of the compounds, the vulcanization curves of the compounds at 160°C are shown in Figure 5.

The compounds can be ranked by increasing scorch times by the filler type: organoclay < carbon black < silica < Na-MMT < non-filler. Various functional groups in the carbon

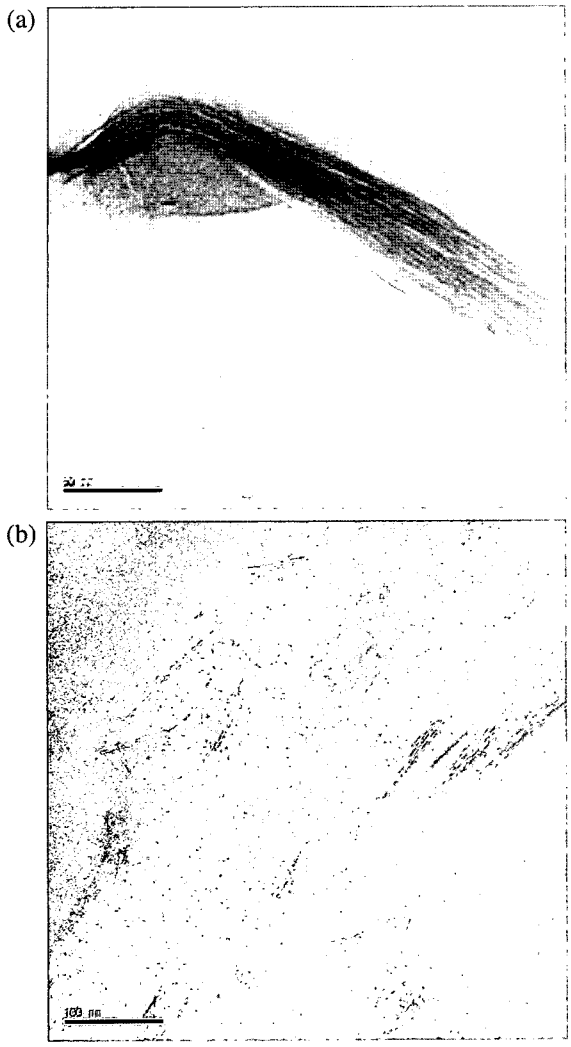

Figure 4. TEM micrographs of (a) Cloisite 15A and (b) the NR/BR nanocomposites.

black in the C2 compound accelerated the curing process. However, the reduction in scorch time and the increase of the cure rate of the C5 compound were significant because the incorporated organoclay contained quaternary alkyl ammonium. It is well known that amines accelerate the curing reaction of rubber. Benzothiazole accelerators when combined with amines produce benzothiazyl anions which accelerate the opening rate of cyclic sulfur.[24]

Na-MMT caused the scorch time of the compound to shorter slightly as compared to the C1 base compound, but the silica filled C3 compound had the third longest scorch time. The compounds can be ranked by increasing maximum torque values by the filler type: non-filler < Na-MMT < silica < organoclay ≅ carbon black. The maximum torque values of Na-MMT filled C4 compound were not high. This is due to the micrometer scale dimensions of the Na-MMT aggregates and poor compatibility between the Na-MMT and the base rubber. However, the organoclay filled C5 compound had high maximum torque values because of the reinforcing effect of fillers and the high crosslink density of compounds. Separation of the layered silicates in the C5 compound introduced better dispersion and a higher aspect ratio of fillers. However, by continuing vulcanization at 160 °C the over-curing reversion was pronounced compared to the carbon black filled C2 compound. This is due to the low thermal stability of the long chain alkyl ammonium ions. The silica filled C3 compound had middle values due to the poor interaction at the filler-matrix interface and the adsorption onto the polar surface of silica and subsequent reduction of the number of accelerators.

To evaluate the effect of the silane coupling agent (Si 69: TESPT) on the cure characteristics of the C5 and C3 compounds, the vulcanization curves at 160 °C are shown in Figure 6. Compared to the C3 compound, the C3-1 compound, which contained the silane coupling agent (TESPT),

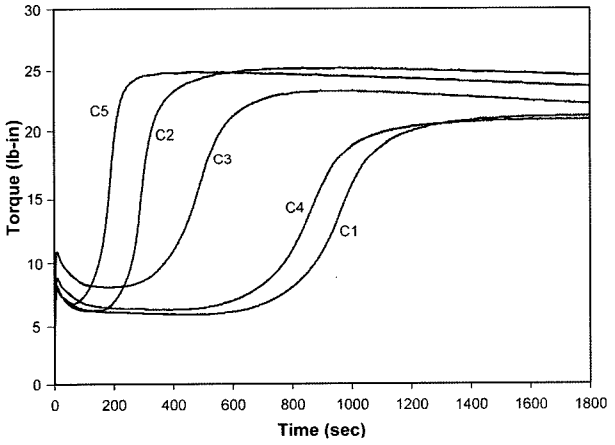

Figure 5. Cure characteristics of the experimental compounds: C1; base, C2; carbon black, C3; silica, C4; Na-MMT, and C5; organoclay filled compounds.

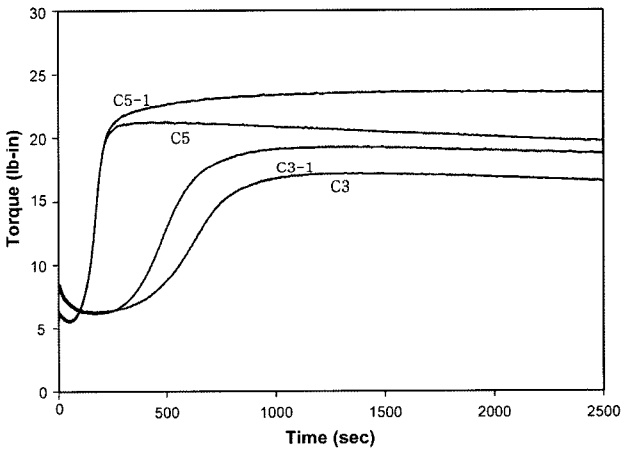

Figure 6. Cure characteristics of the experimental compounds: C3; silica, C3-1; silica (Si 69), C5; organoclay, and C5-1; organoclay (Si 69) filled compounds.

Table II. Mechanical Properties of the Experimental Compounds

	C1	C2	C3	C3-1	C4	C5	C5-1
Modulus 100% (MPa)	0.63	0.85	0.69	0.70	0.69	1.47	1.49
Modulus 300% (MPa)	1.18	1.60	1.33	1.46	1.30	2.47	3.42
Tensile strength (kg_f/cm^2)	10.98	51.08	46.5	48.27	22.57	100.81	86.33
Elongation at break (%)	245	838	1001	879	742	1230	821
Tear energy (kg_f/cm)	3.09	6.19	4.52	7.09	6.37	8.63	7.73
Tension set (%)	-	7.10	25.50	18.06	-	17.65	12.10
Wear rate (mg/rev)	-	0.70	1.23	1.09	-	1.08	0.87

had higher torque values from the beginning of the torque test. This result indicates that matrix-filler bonding by TESPT took place at the silica surface where an abundance of hydroxyl (-OH) groups exist. By the time maximum torque values were achieved, the C5-1 compound had higher torque values than the C5 compound. This result suggests that the major role of TESPT in the C5-1 compound was as an anti-reversion agent, i.e. as a slow sulfur donor.[27] Also this is due to the rare presence of hydroxyl groups, which exist only on the side surfaces of silicates.

Mechanical Properties. In Table II, the mechanical properties of the experimental compounds are shown. The tensile properties are given in terms of modulus on the basis of strain (100 and 300%), tensile strength and elongation at the break.

Organoclay filled C5 & C5-1 compounds had the highest 100 and 300% modulus and tensile strength values, which were due to the separation of clay fillers and the high cross-link density of the compounds. Separation of the clay fillers introduced a high aspect ratio and oriented the fillers to the force direction. This orientation effect was significant when the specimens were greatly elongated. The organoclay filled C5 compound also had the highest tensile strength values, which was due to the large deformation of the compounds. This great elongation at the break was due to molecular slippage on the silicate surface.[12] The Na-MMT filled C4 compound had low modulus and tensile strength values due to the agglomeration of Na-MMT and the poor compatibility between Na-MMT and matrix. The C4 and C5 compounds had high tear energy values, which might have been due to the plate-like shape of Na-MMT and organoclay fillers. The silica filled C3-1 compounds had low modulus and tensile strength values due to the low interaction between the fillers and matrix compared to the carbon black filled C2 compound. Meanwhile, the C3 and C3-1 compounds had relatively high tear energy values which might have been due to the low stress concentration at the crack tip. The low stress concentration was due to the low interaction between filler and matrix resulted in slippage or detachment of polymer molecules from the surface of the fillers.[25] The C3-1 compound, which contained the coupling agent (Si 69), had high 300% modulus and tear energy values compared to the C3 compound. This result might have been due to the modified silica surface, which also resulted in the high dispersion of silica fillers in the matrix. The coupling agent reduced chain slippage on the surface of the fillers by the reaction both of the fillers and matrix, as a result, elongation at the break of the C3-1 and C5-1 compounds decreased as shown in Table II.

Fractional Hysteresis and Permanent Set in the Cyclic Tensile Test. For large deformations, filler-polymer interaction is more important than filler-filler interaction in the dissipation process.

Tensile strength and hysteresis reflect reinforcement and energy dissipation of the C2, C3, C5, and C5-1 compounds and are shown in Figure 7. Each specimen was subject to three tensile cycles. In the first cycle, a specimen was elongated to 100% strain, followed by 5 min of relaxation time. The specimen was allowed to retract to zero stress, and some tensile sets can be seen from this point. The second and third cycles were the same as the first. Hysteresis of the first cycle was much higher than that of the second and the third cycles of the rubber compounds. This is the Mullin effect, which explains the "softening" effect on compounds and thinner loops (less hysteresis) with each cycle.[26]

The organoclay filled C5 & C5-1 compounds had high modulus and hysteresis values compared to the C2 compound. This is due to the orientation of the separated silicate layers and chain sliding of rubber molecules on the silicate surfaces.[12] The chemical bonding of the rubber matrix to the side surfaces of silicates by the coupling agent (TESPT) also leads to a reinforcing effect.

In Figure 8, the fractional hysteresis reported, as the ratio of dissipated energy to applied energy, of the compounds during the cyclic tensile test is shown. Also, tensile set values of the compounds, after the third cycle, are shown in Table II. The carbon black filled C2 compound had the lowest fractional hysteresis and tension set values due to the strong filler-polymer interaction. The silica filled C3 compound had the highest hysteresis and tension set values due to the low interaction between the silica and rubber matrix. The C3-1 and C5-1 compounds containing a coupling agent (TESPT) had low fractional hysteresis and permanent set

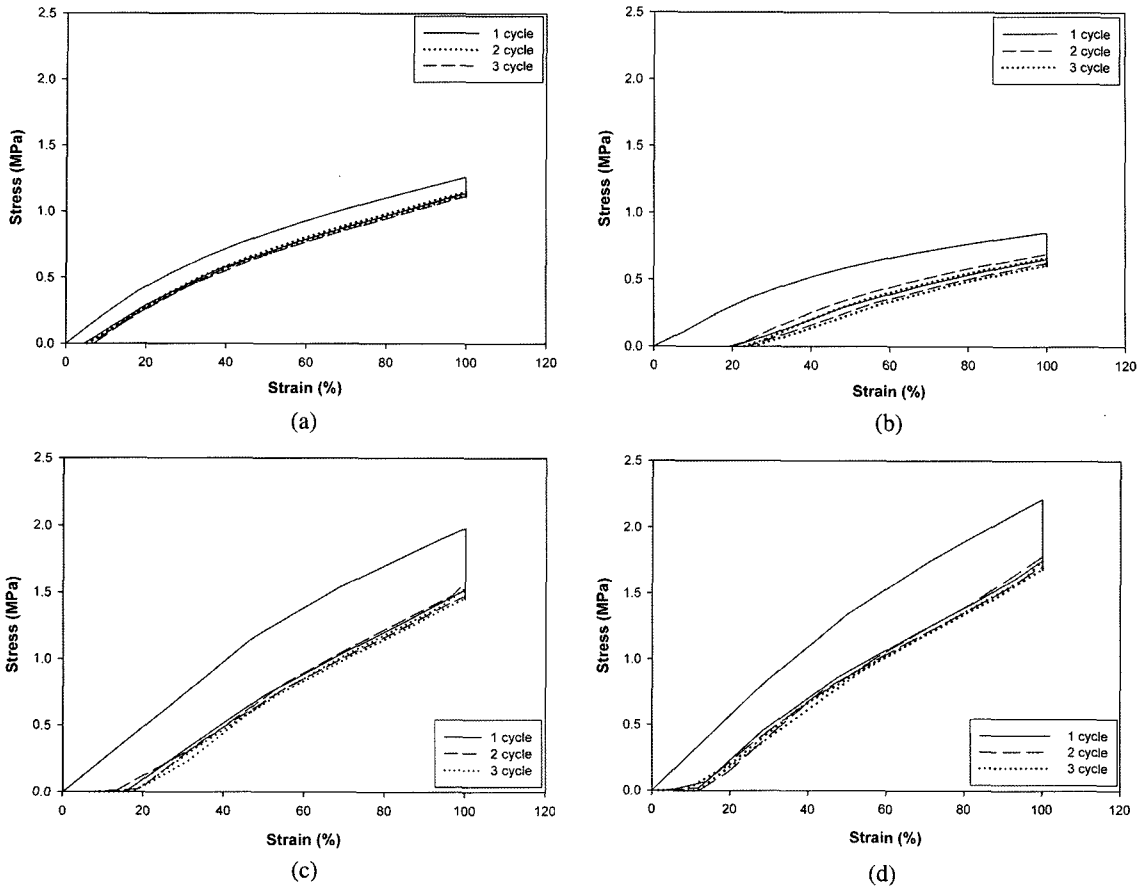

Figure 7. The cyclic tensile test of experimental compounds: (a) C2; carbon black, (b) C3; silica, (c) C5; organoclay, and (d) C5-1; organoclay (Si 69) filled compounds.

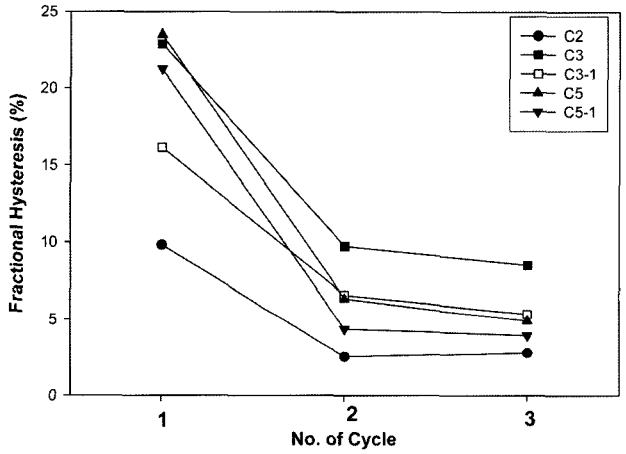

Figure 8. Fractional hysteresis according to the number of cycles for the experimental compounds: C2; carbon black, C3; silica, C3-1; silica (Si 69), C5; organoclay, and C5-1; organoclay (Si 69) filled compounds.

values compared to the C3 and C5 compounds. This is due to the modified surfaces of the silica and silicates by the coupling agent. This modified surface introduces a strong interaction between the fillers and matrix, which dissipates less energy during large deformations. Between the first and second cycle, the extent of fractional hysteresis greatly decreased in the organoclay filled C5 and C5-1 compounds. This is due to the reorientation of the plate-shaped fillers after the first large deformation.[12]

A comparison of the fractional hysteresis and tensile set for each compound after the third cycle can be seen in Figure 8 and Table II. Both values are dependent on the viscous property of vulcanizates. The compounds can be ranked in decreasing order: C3 > C3-1 > C5 > C5-1 > C2. The silica filled compounds had higher energy dissipation values than the organoclay filled compounds. This result suggests that the filler-polymer interaction of the silica filled compounds is weaker than that of the organoclay filled compounds.

Wear Resistance. Table II shows the wear rates of the compounds, which were determined by applying 39.2 Newtons of normal load. The carbon black filled C2 compound had the best wear resistance. This might be due to the strong filler-polymer interaction. The silica filled C3 compound had the worst wear resistance due to its weak filler-polymer

interaction and this might also be due to the low crosslink density of the compound as shown in Figure 5. The organoclay filled C5 compound had medium resistance to wear due to the relatively weak filler-polymer interaction compared to the C2 compound. The silane coupling agent used in the C3-1 and C5-1 compounds improved wear resistance compared to the C3 and the C5 compounds, respectively. This is due to the enhanced dispersion of fillers and improved interfacial strength of the filler-matrix by the modification of the filler surface with the Si-69 coupling agent.

Conclusions

After vulcanization, diffraction peaks reappeared. This might have been due to the escape or rearrangement of long chains of alkyl ammonium, which had been inserted in the galleries of the organoclay. Organoclays in the NR/BR nanocomposites were separated from the original 13~14 layers to the 3~5 layers of silicates. These separated clay fillers caused widespread filler dispersion and a high aspect ratio. The shortened scorch time and the increased cure rate of the C5 and C5-1 compounds were significant due to the incorporation of the quaternary alkyl ammonium ions. The compounds can be ranked in increasing values by maximum torque values in the ODR test as follows: C1<C4<C3<C3-1<C2<C5<C5-1. The 100 and 300% modulus and tensile strength values of the nanocomposites were very consistent with the maximum torque values. The excellent properties of the organoclay filled C5 & C5-1 compounds were due to the high reinforcing effect of the separated clay fillers and the high crosslink density of the compounds. The compounds can be ranked in decreasing order by viscosity as follows: C3>C3-1>C5>C5-1>C2. Fractional hysteresis, tensile set, and wear rate values are very consistent with the viscosity of the vulcanizates. The organoclay filled C5 & C5-1 compounds had high modulus and hysteresis values compared to the C2 compound. This is due to the orientation of the exfoliated silicates and chain sliding of rubber molecules on the silicate surfaces.

Acknowledgements. This work was supported by the Brain Korea 21 Project.

References

(1) A. Usuki, M. Kawasumi, Y. Kojima, A. Okada, T. Kurauchi, and O. Kamigaito, *J. Mater. Res.*, **8**, 1174 (1993).
(2) A. Okada, Y. Kojima, M. Kawasumi, Y. Fukushima, T. Kurauchi, and O. Kamigaito, *J. Mater. Res.*, **8**, 1179 (1993).
(3) S. S. Ray and M. Okamoto, *Progress in Polymer Science*, **28**, 1539 (2003).
(4) Y. T. Vu, J. E. Mark, L. H. Pham, and M. Enhelhardt, *J. Appl. Polym. Sci.*, **82**, 1391 (2001).
(5) S. S. Ray and A. K. Bhowmick, *Rubber Chem. Technol.*, **74**, 835 (2001).
(6) S. Joly, G. Garnaud, R. Ollitrault, L. Bokobza, and J. E. Mark, *Chem. Mater.*, **14**, 4202 (2002).
(7) S. Sadhu and A. K. Bhowmick, *J. Appl. Polym. Sci.*, **92**, 698 (2004).
(8) S. Sadhu and A. K. Bhowmick, *J. Polym. Sci.; Part B: Polym. Phys.*, **42**, 1573 (2004).
(9) M. Arroyo, M. A. Lopez-Manchado, and B. Herrero, *Polymer*, **44**, 2447 (2003).
(10) S. Varghese and J. Karger-Kocsis, *J. Appl. Polym. Sci.*, **91**, 813 (2004).
(11) P. L. Teh, Z. A. Mohd Ishak, A. S. Hashim, J. Karger-Kocsis, and U. S. Ishiaku, *J. Appl. Polym. Sci.*, **94**, 2438 (2004).
(12) M. Ganter, W. Gronski, P. Reichert, and R. Mulhaupt, *Rubber Chem. Technol.*, **74**, 221 (2002).
(13) S. H. Wang, Z. L. Peng, Y. Zhang, and Y. X. Zhang, *Symposium of International Rubber Conference 2004*, Beijing, China, Sep. 21-25, Volume B, pp 257-263.
(14) C. Nah, H. J. Ryu, W. D. Kim, and Y. W. Chang, *Polym. Int.*, **52**, 1359 (2003).
(15) J. T. Kim, T. S Oh, and D. H. Lee, *Polym. Int.*, **52**, 1058 (2003).
(16) N. Hasegawa, H. Okamoto, and A. Usuki, *J. Appl. Polym. Sci.*, **93**, 758 (2004).
(17) H. Zheng, Y. Zhang, Z. Peng, and Y. Zhang, *J. Appl. Polym. Sci.*, **92**, 638 (2004).
(18) J. Ma, P. Xiang, Y. W. Mai, and L. Q. Zhang, *Macromol. Rapid Comm.*, **25**, 1692 (2004).
(19) Y. Q. Wang, H. F. Zhang, Y. P. Wu, J. Wang, and L. Q. Zhang, *Symposium of International Rubber Conference 2004*, Beijing, China, Sep. 21-25, Volume B, pp 420-425.
(20) H. F. Zhang, Y. Q. Wang, Y. P. Wu, L. Q. Zhang, J. Yang, and X. F. Wang, *Symposium of International Rubber Conference 2004*, Beijing, China, Sep. 21-25, Volume B, pp 240-246.
(21) Y. P. Wu, Q. X. Jia, D. S Yu, and L. Q. Zhang, *J. Appl. Polym. Sci.*, **89**, 3855 (2003).
(22) L. Q. Zhang, Y. Z. Wang, Y. Q. Wang, Y. A. Sui, and D. S. Yu, *J. Appl. Polym. Sci.*, **78**, 1873 (2000).
(23) Y. Z. Wang, L. Q. Zhang, C. H. Tang, and D. S. Yu, *J. Appl. Polym. Sci.*, **78**, 1879 (2000).
(24) G. Heideman, R. N. Datta, Z. W. M. Noordermeer, and B. Baarle, *Rubber Chem. Technol.*, **77**, 512 (2004).
(25) M. J. Wang, P. Zang, and K. Mahamud, *Rubber Chem. Technol.*, **74**, 124 (2001).
(26) L. Mullin, *J. Phys. Chem.*, **54**, 239 (1950).
(27) W. W. Barbin and M. B. Rodger, in *Science and Technology of Rubber*, 2nd ed., J. E. Mark, B. Erman, and F. R. Eirich, Eds., Academic Press, New York, 1994, chap. 9, pp 457.